ICARUS **126,** 362–372 (1997)
ARTICLE NO. IS965656

Determination of the Charon/Pluto Mass Ratio from Center-of-Light Astrometry

JEFFREY A. FOUST, J. L. ELLIOT,[1] CATHERINE B. OLKIN,[2] AND STEPHEN W. MCDONALD

Department of Earth, Atmospheric, and Planetary Sciences, Massachusetts Institute of Technology, Room 54-410, Cambridge, Massachusetts 02139-4307
E-mail: jeff@astron.mit.edu

EDWARD W. DUNHAM

Lowell Observatory, 1400 West Mars Hill Road, Flagstaff, Arizona 86001-4499

REMINGTON P. S. STONE

Lick Observatory, Mt. Hamilton, California 95140

JOHN S. MCDONALD

SETI Institute, 2035 Landings Drive, Mountain View, California 94043

AND

RONALD C. STONE

U.S. Naval Observatory Flagstaff Station, PO Box 1149, Flagstaff, Arizona 86002-1149

Received March 19, 1996; revised November 12, 1996

The Charon/Pluto mass ratio is a fundamental but poorly known parameter of the two-body system. Previous values for the mass ratio have ranged from 0.0837 ± 0.0147 (Null *et al.*, 1993, *Astron. J.* 105, 2319–2335) to 0.1566 ± 0.0035 (Young *et al.*, 1994, *Icarus* 108, 186–199). We report here a new determination of the Charon/Pluto mass ratio, using five sets of groundbased images taken at four sites in support of Pluto occultation predictions. Unlike the Null *et al.* and Young *et al.* determinations, where the centers of light for Pluto and Charon could be determined separately, this technique examines the motion of the center of light of the blended Pluto–Charon image. We compute the offsets of the observed center-of-light position of Pluto–Charon from the ephemeris position of the system and fit these offsets to a model of the Pluto–Charon system. The least-squares fits to the five data sets agree within their errors, and the weighted mean mass ratio is 0.117 ± 0.006. The effects of errors in the Charon light fraction, semimajor axis, and ephemeris have been examined and are equal to only a small fraction of the formal error from the fit. This result is intermediate between those of Null *et al.* and Young *et al.* and matches a new value of 0.124 ± 0.008 by Null and Owen (1996, *Astron. J.* 111, 1368–1381). The mass ratio and resulting individual masses and densities of Pluto and Charon are consistent with a collisional origin for the Pluto–Charon system.

INTRODUCTION

The masses of Pluto and Charon provide key information regarding the composition and origin of the two bodies. Given their radii, the densities of the two bodies can be computed. These densities can be used to compute the ratio of rock to ice of each body, providing clues to relative abundances in the outer Solar System. McKinnon (1989) showed that the density of Charon has implications for the origin of the binary system: if Charon has a density of greater than 1.8 g cm^{-3}, the angular momentum density of the binary exceeds the theoretical limit for a stably rotating single object, implying a collisional origin for the system, although a collisional origin is still possible for smaller densities. The masses of Pluto and Charon are also important for refining predictions of stellar occultations by the two bodies: Young *et al.* (1994) point out that a range

[1] Also at Department of Physics, Massachusetts Institute of Technology, and Lowell Observatory.
[2] Now at Lowell Observatory.

0019-1035/97 $25.00

for Charon's density from 1 to 2 g cm^{-3} affects Pluto's shadow path on the Earth by up to half the path's width.

The small ($\leq$1 arcsec) angular separation between Pluto and Charon has made resolved observations of Pluto and Charon difficult: most groundbased images show only a blended image. Millis *et al.* (1989) attempted to make a determination of the mass ratio using blended images of Pluto–Charon taken with a 1.55-m groundbased telescope in support of the 1988 June 9 stellar occultation by Pluto. They noticed a cyclic variation in the location of the center of light with respect to the ephemeris. However, without independent lightcurves for Pluto and Charon, they were unable to fit the variations to a model and solve for the mass ratio.

Null *et al.* (1993) provided the first precise measurement of the mass ratio. Using the Hubble Space Telescope (HST), they resolved Pluto and Charon. By measuring the motion of Pluto and Charon relative to a single background star over 3.2 days (one-half of Charon's orbital period), they computed a Charon/Pluto mass ratio, q, of 0.0837 $\pm$ 0.0147. This mass ratio corresponds to densities of 1.9 to 2.1 g cm^{-3} for Pluto and 1.0 to 1.3 g cm^{-3} for Charon, depending on the radii used.

Young *et al.* (1994) used groundbased observations and a technique that modeled the individual centroids of Pluto and Charon to compute the mass ratio. Pluto–Charon and 10 field stars were observed for six nights (nearly one orbital period of Charon) at the University of Hawaii 2.2-m telescope on Mauna Kea. They modeled the blended Pluto–Charon image as two point sources with numerical point-spread function (PSF) fitting. Using the positions of Pluto, Charon, and the field stars, they determined q to be 0.1566 $\pm$ 0.0035, significantly larger than the Null *et al.* result. This resulted in densities of 1.8 to 2.0 g cm^{-3} for Pluto and 1.8 to 2.3 g cm^{-3} for Charon.

Recently, Null and Owen (1996) reanalyzed their 1991 HST observations with improved field-distortion calibrations. This reanalysis, combined with a new set of HST observations in August 1993, resulted in a revised value for q of 0.124 $\pm$ 0.008. Tholen and Buie (1997), using another HST data set, obtained a mass ratio of $0.110^{+0.063}_{-0.056}$. The wide range in results is evidence that the mass ratio of the Pluto–Charon system is not accurately determined and that further work is needed. This work describes a new attempt to find the mass ratio of the Pluto–Charon system with a more sophisticated version of the Millis *et al.* (1989) approach.

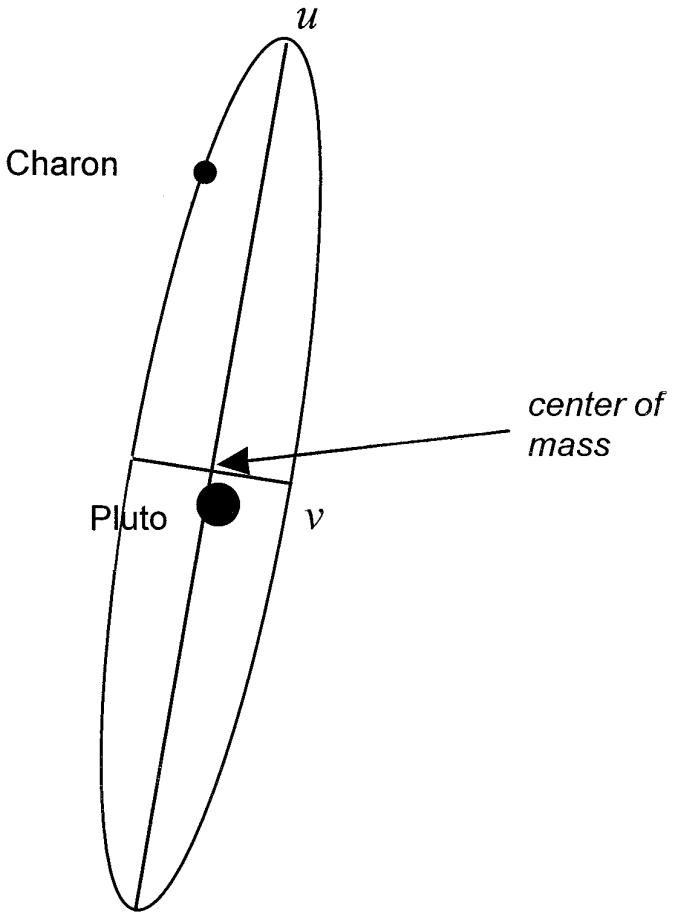

FIG. 1. A representation of the *uv*-coordinate system as applied to Pluto–Charon. The *u*-axis lies along the major axis of Charon's orbit as seen from the Earth, and the *v*-axis lies along the minor axis. The origin of the coordinate system is the barycenter, which is not the same as the mean center-of-light position. The position of Charon is not intended to represent the Pluto–Charon system at a particular time.

MODEL

To find the mass ratio from the periodic motion of the center of light of the system, we must develop a model of the Pluto–Charon binary that will account for this motion with the mass ratio as a free parameter. Fitting this model to positions from our observations of Pluto–Charon will allow us to solve for the mass ratio.

For convenience, we create a model of the Pluto–Charon binary in the *uv* coordinate plane, as discussed by Elliot *et al.* (1993) for Saturn. Here we define the *u*-axis to be aligned with the major axis of Charon's apparent orbit around Pluto and the *v*-axis to be aligned with the minor axis of the apparent orbit (Fig. 1). The origin of the coordinate system is the Pluto–Charon barycenter. This model allows us to compute easily the distance between Pluto and Charon as a function of orbital phase,

$$\Delta u(\varphi) \equiv u_c(\varphi) - u_p(\varphi) = \frac{a}{\Delta}\cos 2\pi\varphi$$
$$\Delta v(\varphi) \equiv v_c(\varphi) - v_p(\varphi) = \frac{a}{\Delta}\sin B \sin 2\pi\varphi, \quad (1)$$

where Δu and Δv represent the offsets along the u and v axes, respectively; $u_p(\varphi)$, $u_c(\varphi)$, $v_p(\varphi)$, $v_c(\varphi)$ are the u- and v-axis positions of Pluto and Charon; a is the semimajor axis of Charon's orbit around Pluto; Δ is the geocentric distance to Pluto (a function of time); φ is the orbital phase in the range 0 to 1, with zero phase defined as the northern elongation of Charon, when v is 0 and u is at a maximum; and B is the latitude of the sub-Earth point on Pluto. The time of northern elongation and values for the latitude of the sub-Earth point on Pluto came from the *Astronomical Almanac* for the appropriate year. The orbital period of Charon, 6.387246 ± 0.000011 days, is from Tholen and Buie (1990) and is consistent with the more recent result of 6.387223 ± 0.000017 days (Tholen and Buie 1997). We assume that the orbit of Charon has zero eccentricity, based on limits placed by Tholen and Buie (1990), which allows us to compute easily φ for any time. Recent observations (Tholen and Buie 1997) indicate that Charon's orbit may have an eccentricity of 0.0076 ± 0.0005. Including this eccentricity in our calculations changes our results by less than 1% of our error.

If we know the positions of Pluto and Charon and the fraction of the total system light, $f_\ell(\varphi)$, that comes from Charon as a function of phase, we can compute the instantaneous center-of-light position $u_\ell(\varphi)$, $v_\ell(\varphi)$ of the Pluto–Charon system:

$$\begin{aligned} u_\ell(\varphi) &= [1 - f_\ell(\varphi)]u_p(\varphi) + f_\ell(\varphi)u_c(\varphi) \\ v_\ell(\varphi) &= [1 - f_\ell(\varphi)]v_p(\varphi) + f_\ell(\varphi)v_c(\varphi). \end{aligned} \tag{2}$$

These equations assume that the center of light corresponds to the center of mass of the body. The effects of albedo variations on Pluto and Charon on this relationship are discussed later in this paper.

Similarly, given the system mass fraction of Charon f_m, we can find the location of the barycenter of the system from the positions of Pluto and Charon:

$$0 = [1 - f_m]u_p(\varphi) + f_m u_c(\varphi). \tag{3}$$

The equation for the v-axis is identical and is not shown here and in future calculations. The Charon mass fraction f_m is related to the Charon/Pluto mass ratio q by the equation

$$f_m = \frac{q}{1+q}. \tag{4}$$

By subtracting Eq. (3) from Eq. (2), we can find the position of the center of light of the system as a function of the mass fraction, and hence the mass ratio, thus

$$u_\ell(\varphi) = [f_\ell(\varphi) - f_m][u_c(\varphi) - u_p(\varphi)], \tag{5}$$

or, noting that the $u_c(\varphi) - u_p(\varphi)$ term is simply the distance between Charon and Pluto,

$$u_\ell(\varphi) = [f_\ell(\varphi) - f_m]\,\Delta u(\varphi). \tag{6}$$

Since we cannot directly determine $u_\ell(\varphi)$ without knowing the mass fraction, we need an alternate method of obtaining the position of the center of light. The Pluto ephemeris corresponds to the mean position of the center of light, since it is based on unresolved astrometric images. We can subtract the center of light at any phase from the mean position with the result

$$u_{\ell\bar{\ell}} \equiv \bar{u}_\ell - u_\ell(\varphi) = \bar{u}_\ell - [f_\ell(\varphi) - f_m]\,\Delta u(\varphi). \tag{7}$$

Moreover, we can compute the mean value of u from the definition of the center of light:

$$\bar{u}_\ell = \int_0^1 u_\ell(\varphi)\, d\varphi. \tag{8}$$

This approach requires that we make an initial estimate of the mass ratio; however, the final result is insensitive to the starting value used. We can now solve Eq. (7) for f_m and thus q. This approach requires that we convert the offsets from the *fg* plane (Elliot *et al.* 1993), a plane centered on the barycenter with f pointing in the direction of increasing right ascension and g in the direction of increasing declination, to the *uv* plane. A rotation matrix is used for the conversion,

$$\begin{bmatrix} u \\ v \end{bmatrix} = \begin{bmatrix} \cos P & -\sin P \\ \sin P & \cos P \end{bmatrix} \begin{bmatrix} f \\ g \end{bmatrix}, \tag{9}$$

where P is the position angle of Pluto's north pole, as defined by the direction of the angular momentum vector of the planet, from the *Astronomical Almanac*.

DATA ANALYSIS

Observations

The first set of Pluto–Charon positions came from observations in September and October 1993 from the 0.91-m Crossley telescope at Lick Observatory in California. Strip scans of Pluto–Charon and a network of field stars were taken in a longpass filter with a modified clone of the original SNAPSHOT camera (Dunham 1995) in support of the P20 occultation prediction effort (Olkin *et al.* 1993). Altogether, 49 scans were taken over 11 nights.

A similar effort was undertaken from May through July 1995 for the prediction of the P28 occultation. Strip scans of Pluto–Charon and a network of field stars were recorded at Lick Observatory from May 28 through July 9 in the V

TABLE I
Summary of Observations

Observatory	Dates	Type	Filter	No. of observations
Lick Observatory (Crossley 0.91-m)	1993 September 13–1993 October 5	Strip scan	*V*	49
Lick Observatory (Crossley 0.91-m)	1995 May 28–1995 July 9	Strip scan	*V*	135
Wallace Observatory (0.61-m)	1995 May 6–1995 July 4	Strip scan	Open[a]	222
CAMC	1989 February 16–1995 April 6	Transit telescope	*V*	220
USNO FASTT	1995 March 13–1995 July 12	Transit telescope	*V*	21

[a] Approximately *R* (Dunham *et al*. 1991).

filter using the Crossley 0.91-m telescope and the modified SNAPSHOT. Strip scans were taken at Wallace Astrophysical Observatory in Massachusetts from May 6 through July 4, with the 0.61-m telescope and the observatory's original SNAPSHOT camera (Dunham *et al.* 1985). To obtain sufficient signal, no filter was used in the Wallace observations. The unfiltered light closely approximates the *R* passband for most stars (Dunham *et al.* 1991). Altogether, 135 scans over 20 nights were taken at Lick and 222 scans over 23 nights were taken at Wallace.

An additional source of Pluto–Charon center-of-light positions was meridian circle observations. The U.S. Naval Observatory Flagstaff Astrometric Scanning Transit Telescope (FASTT) (Stone 1993, Stone *et al.* 1996) obtained 21 Pluto positions for the P28 prediction effort between 1995 March 13 and July 12. Also, the Carlsberg Automatic Meridian Circle (CAMC) on La Palma provided 220 Pluto positions from 1989 through 1995. These observations were taken as a part of their ongoing campaign to improve Pluto's ephemeris (Carlsberg 1988–1993). A summary of all observations used in this analysis is shown in Table I.

Reductions

Strip scans from Lick and Wallace Observatories were processed through a software "pipeline" developed for processing data from occultation candidate searches and prediction efforts (Dunham *et al.* 1991, McDonald and Elliot 1992, McDonald and Elliot 1995). Each strip was flattened and then processed with DAOPHOT (Stetson 1987) to identify all the stars on the strip that were within a certain ADU range, avoiding stars without sufficient signal or stars that were in the nonlinear regime of the CCD. The star positions on the strips were fitted by linear registration to an astrometric reference network of 95 stars (1993 data) and 157 stars (1995 data) whose positions had been determined by CAMC. These fits provided the right ascension and declination of the stars on the strip and the center-of-light position of Pluto.

The center-of-light positions for Pluto–Charon and the stars fluctuate, or "wobble" from image to image, due to changes in the gross atmospheric refraction as the strip scan is exposed (Dunham *et al.* 1991). Figure 4 of that paper shows the low-frequency undulations in the offsets between the observed position of a star and the mean position of the star in five strip scans. This wobble was corrected by finding the difference between the centers of stars in a standard coordinate system to a network of approximately 400 stars (1993 data) and 2000 stars (1995 data) whose mean positions had been accurately determined by averaging over a large number of strip scans. The wobble was modeled by a Fourier series, which matches the variations in position well, and then removed from the standard stars and Pluto–Charon. An additional correction was applied to the 1995 Lick data to remove a distortion in the focal plane of the telescope (Dunham *et al.* 1994).

Data from the USNO transit telescope and the Carlsberg Automatic Meridian Circle were provided in the form of lists of Pluto–Charon center-of-light positions (J2000 equinox), and no additional processing was required.

Analysis Technique

We used the *Mathematica* software package (Wolfram 1991) to construct the model of the Pluto–Charon binary and fit it to the observed positions of the system. First, the observed center-of-light positions of Pluto–Charon, computed as described above, were transformed from topocentric to geocentric coordinates so they could be directly compared with the ephemeris positions. The offsets between the DE211 ephemeris (Standish 1994) position of Pluto at the time of each observation and the corresponding center-of-light position were then computed.

The resulting offsets fit long-term linear trends due to a fixed rotation of the ephemeris system with respect to the network system (less than half an arcsecond over the span of the observations—see Fig. 2). To compensate for these trends, we fit first- and second-order polynomials to each data set and subtracted the polynomial from the offset values. In each case the second-order term, which was used to check for any nonlinearity in the rotation, was small, and its inclusion had no effect on the mass ratio solution.

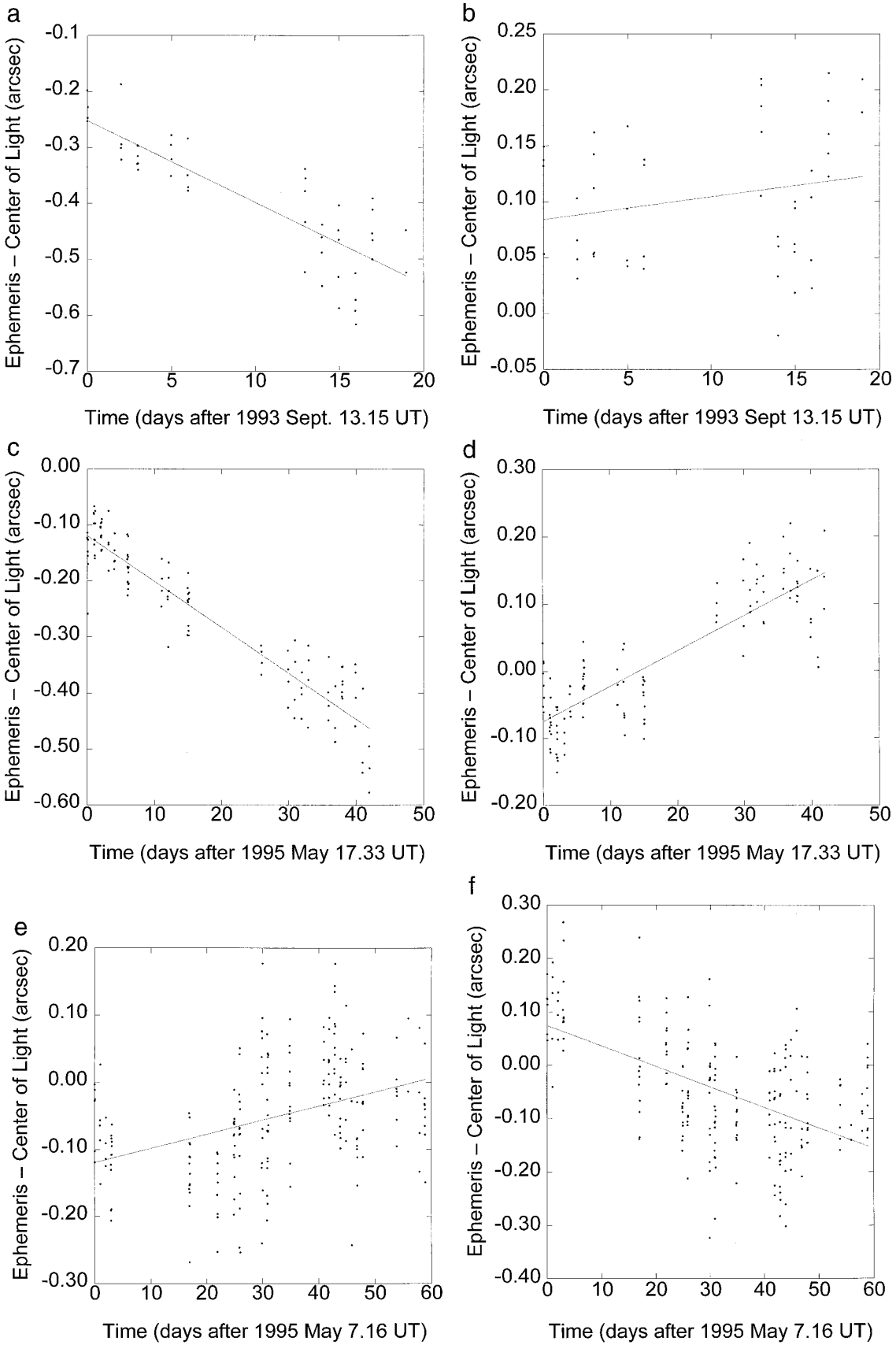

FIG. 2. Offsets between the ephemeris and center-of-light positions for the 1993 Lick, 1995 Lick, and 1995 Wallace data sets. Least-square best-fit lines have been plotted for each data set. (a) The offset in right ascension for the 1993 Lick data. (b) The offset in declination for the 1993 Lick data. (c) The offset in right ascension for the 1995 Lick data. (d) The offset in declination for the 1995 Lick data. (e) The offset in right ascension for the 1995 Wallace data. (f) The offset in declination for the 1995 Wallace data.

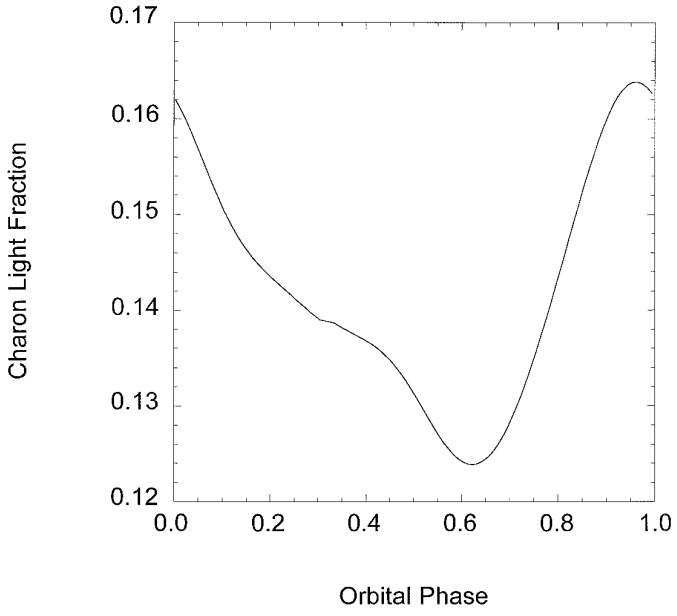

FIG. 3. The Charon light fraction as a function of its orbital phase from Buie *et al.* (1997). The mean value of the light fraction is 0.142. The zero-phase time is defined as the first northern elongation of 1980.

The new offsets were then transformed into the *uv*-plane by Eq. (9).

To compare the observed offsets with the theoretical offsets from the model, we used the Charon light fraction $f_\ell(\varphi)$ as a function of orbital phase created from lightcurve data (Buie *et al.* 1997, see Fig. 3 in this paper). The zero-phase time of this function is based on the time of northern elongation. We also used a mean value of this function and a light fraction function that assumed a constant magnitude for Charon (Fig. 3) for separate determinations of the mass ratio. The functions were then combined with the position of Charon with respect to Pluto (Eq. (1)), the Charon mass fraction, and the mean center-of-light position (Eq. (8)) to form the function for the offset between the mean and observed values of the center of light (Eq. (7)). This model was fit to the offsets with least-squares. Both the *u*- and the *v*-axis equations were fit simultaneously, with the mass fraction (expressed as a function of the mass ratio, using Eq. (4)) as the only free parameter. This technique resulted in a best-fit value for the mass ratio and its formal error. Figure 4 shows the offsets in the data with the offsets generated by the best-fit model. The mass ratio values and their errors are shown in Table II and are discussed in detail below.

RESULTS

Table II lists the mass ratio results for the five data sets. The second column lists the number of positions used in the fit. A total of 121 of the 135 1995 Lick strips and 217 of the 222 Wallace strips provided useful Pluto–Charon center-of-light positions; the remainder were discarded due to a lack of astrometric standard stars visible in the image or (on one night of Lick data) a merged Pluto–Charon–star image that provided unreliable center-of-light positions. The third column lists the standard deviation of the offsets in right ascension and declination between the ephemeris and center-of-light positions, which shows the scatter in the positions. Note that the transit telescope observations have a scatter up to five times as large as for the strip scan positions. We believe that this difference is observed because the wobble in the position of Pluto (Dunham *et al.* 1991) has been removed from the strip scan data but not from the transit telescope data, hence eliminating much of the scatter. The fourth column lists the best-fit mass ratio using the Buie *et al.* (1997) light fraction function, the fifth column lists the mass ratio using the mean value of the Buie *et al.* light fraction, $\bar{f}_\ell = 0.142$, as a constant value for the light fraction, and the sixth column lists the mass ratio using a value of the mass ratio using a light fraction function that uses a constant value for Charon's magnitude. While the transit telescope values are high, all the results are consistent with one another within their errors.

Investigation of Possible Systematic Errors

Although the mass ratio is fairly insensitive to the use of the Charon light fraction function versus the mean value of the function, possible systematic errors in the light fraction function and semimajor axis of Charon's orbit around Pluto may have a more substantial influence on the value of the mass ratio. To investigate this possibility, we solved Eq. (6) for q:

$$q = \frac{\Delta u_\ell(\varphi) f_\ell(\varphi) - u_\ell(\varphi)}{\Delta u_\ell(\varphi)(1 - f_\ell(\varphi)) + u_\ell(\varphi)}. \tag{10}$$

We then took partial derivatives of q with respect to a and $f_\ell(\varphi)$:

$$\frac{\partial q}{\partial f_\ell(\varphi)} = \frac{\Delta u_\ell^2(\varphi)}{(\Delta u_\ell(\varphi)(1 - f_\ell(\varphi)) + u_\ell(\varphi))^2} \tag{11a}$$

$$\frac{\partial q}{\partial a} = \frac{u_\ell(\varphi)\,\Delta \cos 2\pi\varphi}{((f_\ell - 1)a \cos 2\pi\varphi - u_\ell(\varphi)\,\Delta)^2}. \tag{11b}$$

Using the errors on the Pluto and Charon magnitudes from Buie *et al.* (1997), we found the average error in the Charon light fraction to be 0.0013. Using Eq. (11a) and appropriate values for $u_\ell(\varphi)$, $\Delta u_\ell(\varphi)$, and $f_\ell(\varphi)$, we found the resulting error in the mass ratio from this source to be 0.0016. This value is much smaller than the errors in the fits from any of the data sets, so we can conclude that

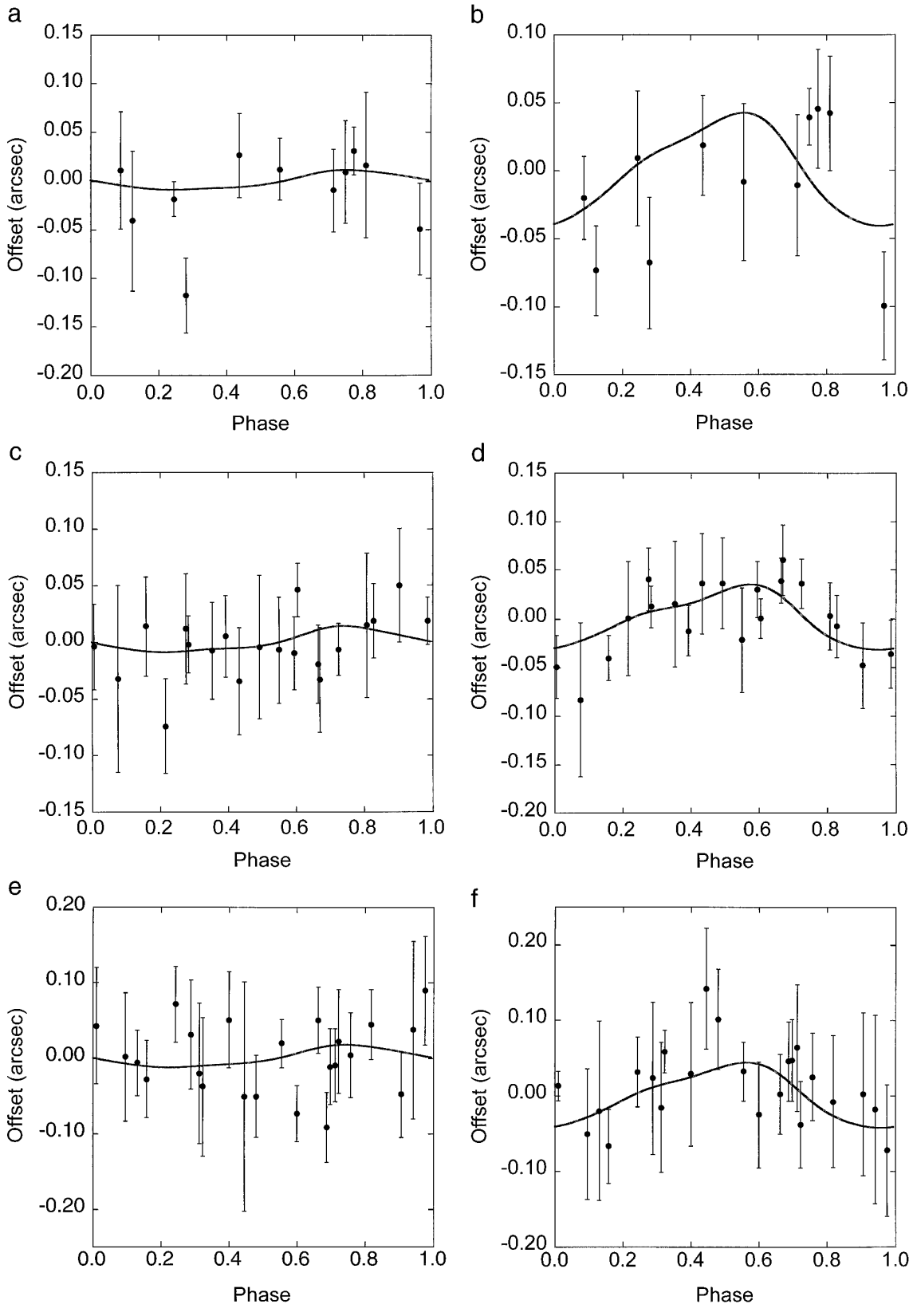

FIG. 4. A comparison of model offsets with data offsets. Each data point (black circles) represents a mean offset for that night, and the error bars are the standard deviation from the nightly averages. Long-term trends (Fig. 2) have been removed from these positions. The line shows the positions from the best-fit model. The *x*-axis for all the figures is orbital phase. (a) Right ascension offsets for the 1993 Lick data. (b) Declination offsets for the 1993 Lick data. (c) Right ascension offsets for the 1995 Lick data. (d) Declination offsets for the 1995 Lick data. (e) Right ascension offsets for the 1995 Wallace data. (f) Declination offsets for the 1995 Wallace data.

TABLE II
Summary of Mass Ratio Results

Data set	No. of positions	Standard deviation of offsets (arcsec)[a] RA	Dec	Mass ratio (light fraction function)	Mass ratio (mean light fraction)	Mass ratio (light fraction function using mean Charon)
Lick 1993	49	0.060	0.061	0.097 ± 0.018	0.101 ± 0.018	0.098 ± 0.018
Lick 1995	121	0.044	0.050	0.122 ± 0.007	0.118 ± 0.007	0.123 ± 0.007
Wallace 1995	217	0.080	0.092	0.107 ± 0.011	0.102 ± 0.011	0.107 ± 0.011
CAMC 1989–1995	220	0.289	0.221	0.154 ± 0.034	0.152 ± 0.034	0.155 ± 0.034
USNO 1995	21	0.156	0.202	0.189 ± 0.077	0.186 ± 0.077	0.187 ± 0.077

[a] For an individual measurement.

errors in the Charon light fraction are not a significant source of error in the determination of the mass ratio.

For the semimajor axis, Beletic *et al.* (1989) found a solution of $a = 19640 \pm 320$ km, which has been confirmed to higher precision with values of 19662 ± 81 km by Null and Owen (1996) and 19636 ± 8 km by Tholen and Buie (1997), although the potential error due to albedo markings on Pluto and Charon may be as large as 30 km. However, Young *et al.* (1994) found $a = 19460 \pm 58$ km, which is not consistent with the other values, although Tholen and Buie (1997) speculate that this value may be due to an implicit weighting of data from the Young *et al.* analysis toward the periapsis of Charon's orbit around Pluto. Using the largest error from these estimates (320 km) in Eq. (11b) with appropriate values for $a, \Delta, f_\ell(\varphi)$, and $u_\ell(\varphi)$, we found the corresponding average error in the mass ratio is 0.0011, or only somewhat more than half of error induced by the uncertainty in the light fraction. Thus, the uncertainty in the semimajor axis of Charon's orbit is not a significant source of error in the determination of the mass ratio.

In our calculations we assume that both Pluto and Charon are featureless disks with no albedo variations. However, analyses of mutual event observations (Buie *et al.* 1992, Young and Binzel 1993) have shown that both bodies do have significant albedo variations over their surfaces. These variations can alter the location of the center of light of each body, changing the center of light of the blended image. These variations can be as large as 100 km on Pluto and 20 km on Charon, both in the longitudinal direction (roughly corresponding to declination), with considerably smaller variations in the latitudinal direction, depending on the model used (M. Buie, private communication). At Pluto–Charon's distance from the Earth, albedo variations can produce a variation of approximately 5 marcsec in the center-of-light position on the sky. The amplitude of the declination offsets from the best-fit models is 40 marcsec.

Current albedo maps are not accurate enough to generate a correction to the offset (M. Buie, private communication), so we cannot remove this variation from our analysis. The maximum-entropy maps are accurate only for the Charon-facing side of Pluto. Moreover, the maps are light contours with no information on the placement of the coutours with respect to the geometrical center of the planet or its center of mass. These limitations of current albedo maps make them unsuitable for this work.

Instead, we attempted to model the magnitude of this effect by introducing a sinusoidal variation in the center-of-light position of the model of amplitude 4 marcsec (100 km). This modification changed the mass ratio for all five data sets by ± 0.001–0.002, depending on the phase of the sinusoid function. In all cases the offset is considerably smaller than the errors in the fit. By comparison, Null and Owen (1996) report that their value of q decreases by 0.002 if the albedo correction is removed, a difference similar to our results.

All the mass ratio determinations above rely on the use of an accurate ephemeris for Pluto to determine the center-of-light offsets in the data. To test the dependence of the mass ratio on the ephemeris, we used three recent Pluto ephemerides: DE211, DE245, and DE403. Right ascension and declination offsets for these ephemerides for the 1993 and 1995 data sets are shown in Table III. The differences in the value of the mass ratio for the DE245 and DE403 ephemerides was very small: less than 1% for all three data sets. The change in geocentric Pluto distances among these ephemerides is less than 10^{-4} AU, which has no impact on the solution. We conclude that any of these ephemerides is suitable for this analysis.

DISCUSSION

Figure 5 shows the mass ratios and associated errors from the various data sets, using both the Buie *et al.* Charon light fraction function and the mean value of the Charon

TABLE III
Offsets between the DE211, DE245, and DE403 Ephemerides

	Right ascension offsets (arcsec)		Declination offsets (arcsec)	
Ephemerides	1993	1995	1993	1995
DE245-DE211	0.242	0.323	−0.004	−0.014
DE403-DE211	0.057	0.030	0.078	0.074

light fraction. The figure shows that these results are consistent within their errors. The weighted mean of the mass ratios is $q = 0.117 \pm 0.006$ using the light-fraction function, $q = 0.114 \pm 0.006$ using the mean light fraction, and $q = 0.118 \pm 0.006$ using the light-fraction function with a mean Charon magnitude. We feel that the analysis with the full light-fraction function should be closest to reality and therefore we adopt 0.117 ± 0.006 as our value for the mass ratio.

This new value for the mass ratio allows us to compute the individual masses of Pluto and Charon. We adopt a mass for the Pluto–Charon system of $1.472 \pm 0.072 \times 10^{25}$ g (Tholen and Buie 1990), which is consistent with the value (19640 ± 320 km) of the semimajor axis of Charon's orbit adopted for our analysis. This result also spans the estimates of $1.420 \pm 0.019 \times 10^{25}$ g (Null *et al.* 1993) and $1.432 \pm 0.013 \times 10^{25}$ g (Young *et al.* 1994) which used smaller values for a. This system mass provides Pluto and Charon masses as shown in Table IV.

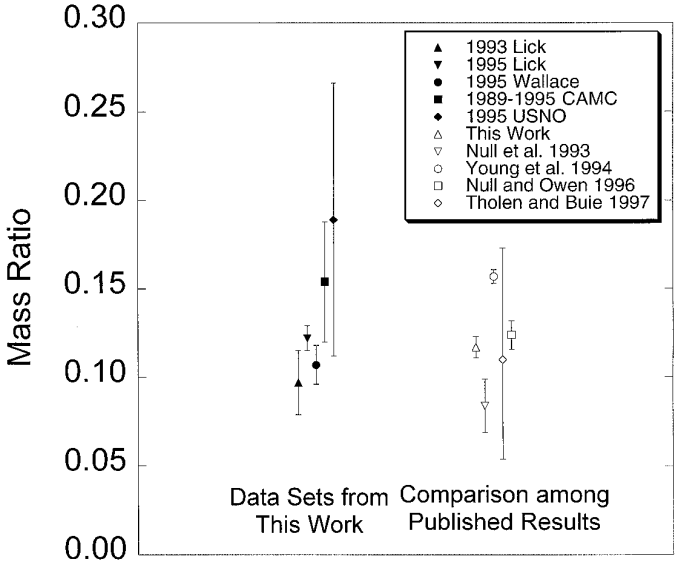

FIG. 5. A comparison of the mass ratios from data sets in this work and from other published results. The left-hand side of the figure shows the various mass ratio results from data sets used in this analysis, using the adopted solution of the Buie *et al.* (1997) lightcurves. Note that despite the high values of the transit circle data, all the results are consistent within their error bars. The right-hand side compares mass ratio results reported in other works. The point labeled "This Work" refers to the weighted mean of the values on the left-hand side of the plot. Our result compares favorably with the work of Null and Owen (1996) and is intermediate between the results of Null *et al.* (1993) and Young *et al.* (1994).

For the densities of Pluto and Charon, we used the masses computed above and estimates of the radii of the two bodies. Published radii for Pluto range from 1151 ± 6 km (Tholen and Buie 1990) to 1195 ± 5 km (Elliot and Young 1992). Published radii for Charon range from 593 ± 13 km (Tholen and Buie 1990) to 642 ± 11 km (Young 1992) and 650 km (Albrecht *et al.* 1994). We have adopted estimates that span the given ranges: a radius of 1175 ± 25 km for Pluto and 620 ± 30 km for Charon. The resulting densities are shown in Table IV.

We can use these densities to compute a rough estimate of the rock and ice fractions of Pluto and Charon, using the relationship from Simonelli *et al.* (1989):

$$\frac{1}{\bar{\rho}} = \frac{X_R}{\rho_R} + \frac{1 - X_R}{\rho_I} \tag{12}$$

Here, X_R is the rock mass fraction, $\bar{\rho}$ is the mean density of the body, and ρ_R and ρ_I are the rock and ice densities, respectively. We set the ice density to 1 g cm^{-3} and the rock density to 3 g cm^{-3} and ignored differences in density among different types of rock or ice or changes in density of rock and ice caused by differences in pressure. The resulting rock mass fractions are shown in Table IV.

To compare our results with previous work, we applied the mass ratios from Null *et al.* (1993), Young *et al.* (1994), and Null and Owen (1996) to the same system mass and radii as above. The results are displayed in Table IV.

The results above show that although there are significant differences in the mass of Pluto, its density is constrained to approximately 1.9 to 2.0 g cm^{-3}. However, there is nearly a factor of two difference in the value of the density of Charon due to a similar difference in the mass of Charon. The mass and density of Charon are much more sensitive to small changes in the Charon/Pluto mass ratio because of the mass ratio's low value.

These results have implications on the composition and origin of the Pluto–Charon system. McKinnon (1989) showed that if Charon's density exceeds 1.8 g cm^{-3}, no solution for a stable-rotating single body exists, implying that Charon was formed by a collision between Pluto and another body. From Table IV, only the Young *et al.* mass ratio produces a Charon density in excess of 1.8 g cm^{-3}, although the mass ratio from the light fraction function and the Null and Owen mass ratio produce Charon densities within 1-σ of the critical value. However, even using the smallest densities of Charon from the above tables,

TABLE IV
Comparison of Bulk Properties for Pluto and Charon

	Null *et al.* (1993)	Young *et al.* (1994)	Null and Owen (1996)	This work
Mass ratio	0.084 ± 0.015	0.157 ± 0.004	0.124 ± 0.008	0.117 ± 0.006
Pluto mass (10^{24} g)	13.58 ± 0.19	12.73 ± 0.10	13.10 ± 0.12	13.18 ± 0.10
Charon mass (10^{24} g)	1.14 ± 0.19	1.99 ± 0.10	1.62 ± 0.12	1.54 ± 0.10
Pluto density (g cm^{-3})	2.00 ± 0.13	1.87 ± 0.12	1.93 ± 0.12	1.94 ± 0.12
Charon density (g cm^{-3})	1.14 ± 0.25	2.00 ± 0.31	1.63 ± 0.27	1.54 ± 0.25
Pluto rock fraction	0.75 ± 0.05	0.70 ± 0.05	0.72 ± 0.05	0.73 ± 0.05
Charon rock fraction	0.19 ± 0.30	0.75 ± 0.12	0.58 ± 0.15	0.53 ± 0.16

Note. Masses, densities, and rock fractions based on a system mass of $1.472 \pm 0.072 \times 10^{25}$ g, a Pluto radius of 1175 ± 25 km, and a Charon radius of 620 ± 30 km.

the normalized angular momentum density of the system (McKinnon 1989) is still more than twice that for the Earth–Moon system, which current theories suggest has a collisional origin (Stevenson 1987).

Charon's smaller density and rock fraction provide additional evidence for a collisional origin for the system. McKinnon (1989) points out that an icier Charon would be analogous to the Moon, which may have been formed in a collision between a differentiated Mars-sized object with a differentiated proto-Earth. This collision resulted in the formation of a body—the Moon—without heavy metals and thus with a lower density than the Earth. If either the proto-Pluto or the colliding body was differentiated, the collision could result in the formation of a body with more ice and a corresponding lower density than Pluto. Stern (1988) uses energy considerations to argue that Pluto must be differentiated if its density is greater than 1.6 g cm^{-3}, a condition satisfied by all the mass ratios presented above. Models of a differentiated Pluto also exist for the range of computed Pluto rock mass fractions (McKinnon and Mueller 1988, Simonelli and Reynolds 1989).

CONCLUSIONS

Based on center-of-light astrometry obtained from Lick and Wallace Observatories, we have found a weighted mean Charon/Pluto mass ratio q of 0.117 ± 0.006 using the Charon light fraction function derived from Buie *et al.* (1997). These mass fractions imply a Pluto mass of approximately $1.32 \pm 0.01 \times 10^{25}$ g and a Charon mass of $1.5 \pm 0.1 \times 10^{24}$ g. They also imply a Pluto density of 1.94 ± 0.12 g cm^{-3} and a Charon density of 1.5 ± 0.2 g cm^{-3}, with corresponding rock fractions of 0.73 ± 0.05 for Pluto and 0.53 ± 0.16 for Charon.

The mass ratios found compare favorably with the recent results of Null and Owen (1996), who determined q = 0.124 ± 0.008 (Fig. 5). This consistency suggests that we are approaching consensus on the individual masses of Pluto and Charon. Future work, using different data sets and/or different techniques, should be conducted to verify these results. As the error in the densities and rock mass fractions of the two bodies are controlled by the error in their radii, these quantities are unlikely to be improved until the radii of the two bodies are better known and we understand their interior structures.

ACKNOWLEDGMENTS

We thank Michael Buontempo for providing the CAMC Pluto position data; Chuck Ford, Arno Granados, Laurance Doyle, and Leslie Young for their work providing Lick observations; and Michael Mattei for providing Wallace observations. We also thank David Tholen and an anonymous reviewer for numerous useful comments and suggestions. This work was supported in part by NASA Grant NAGW-1494.

REFERENCES

Albrecht, R., C. Barbieri, H.-M. Adorf, G. Corrain, A. Gemmo, P. Greenfield, O. Hainaut, R. N. Hook, D. J. Tholen, J. C. Blades, and W. B. Sparks 1994. High-resolution imaging of the Pluto–Charon system with the Faint Object Camera of the Hubble Space Telescope. *Astrophys J.* **435,** L75–L78.

Beletic, J. W., R. M. Goody, and D. J. Tholen 1989. Orbital elements of Charon from speckle interferometry. *Icarus* **79,** 38–46.

Buie, M. W., D. J. Tholen, and K. Horne 1992. Albedo maps of Pluto and Charon—Initial mutual event results. *Icarus* **97,** 211–227.

Buie, M. W., D. J. Tholen, and L. H. Wasserman 1997. Separate lightcurves of Pluto and Charon. *Icarus* **125,** 233–244.

Carlsberg Meridian Catalogues 5–8 (1988–1993), Copenhagen University Observatory, Royal Greenwich Observatory, Real Instituto y Observatorio de la Armada en San Fernando.

Dunham, E. W. 1995. Optical instrumentation for airborne astronomy. In *Proceedings of the Airborne Astronomy Symposium on the Galactic Ecosystem: From Gas to Stars to Dust* (M. R. Haas, J. A. Davidson, and E. F. Erickson, Eds.). ASP, San Francisco.

Dunham, E. W., R. L. Baron, J. L. Elliot, J. V. Vallerga, J. P. Doty, and G. R. Ricker 1985. A high-speed, dual-CCD imaging photometer. *Publ. Astron. Soc. Pacific* **97,** 1196–1204.

Dunham, E. W., C. H. Ford, R. P. S. Stone, S. W. McDonald, C. B. Olkin, and J. L. Elliot 1994. Occultation predictions using CCD strip-scanning astrometry. *Bull. Am. Astron. Soc.* **26,** 1154.

Dunham, E. W., S. W. McDonald, and J. L. Elliot 1991. Pluto–Charon stellar occultation candidates: 1990–1995. *Astron. J.* **102,** 1464–1484.

Elliot, J. L., A. S. Bosh, M. L. Cooke, R. C. Bless, M. J. Nelson, J. W. Percival, M. J. Taylor, J. F. Dolan, E. L. Robinson, and G. W. van Citters 1993. An occultation by Saturn's rings on 1991 October 2–3 observed with the Hubble Space Telescope. *Astron. J.* **106,** 2544–2572.

Elliot, J. L., and L. A. Young 1992. Analysis of stellar occultation data for planetary atmospheres. I. Model fitting, with application to Pluto. *Astron. J.* **103,** 991–1015.

McDonald, S. W., and J. L. Elliot 1992. Triton stellar occultation candidates: 1992–1994. *Astron. J.* **104,** 862–879.

McDonald, S. W., and J. L. Elliot 1995. Triton stellar occultation candidates: 1995–1999. *Astron. J.* **109,** 1352–1362.

McKinnon, W. B. 1989. On the origin of the Pluto–Charon binary. *Astrophys. J.* **344,** L41–L44.

McKinnon, W. B., and S. Mueller 1988. Pluto's structure and composition suggest origin in the solar, not a planetary, nebula. *Nature* **335,** 240–243.

Millis, R. L., L. H. Wasserman, O. G. Franz, C. C. Dahn, and A. R. Klemola 1989. The mass ratio of the Pluto/Charon system. *EOS* **70,** 381–382.

Null, G. W., and W. M. Owen, Jr. 1996. Charon/Pluto mass ratio obtained with HST CCD observations in 1991 and 1993. *Astron. J.* **111,** 1368–1381.

Null, G. W., W. M. Owen, and S. P. Synnott 1993. Masses and densities of Pluto and Charon. *Astron. J.* **105,** 2319–2335.

Olkin, C. B., S. W. McDonald, and J. L. Elliot 1993. Pluto. *IAUC* 5872.

Simonelli, D. P., J. B. Pollack, C. P. McKay, R. T. Reynolds, and A. L. Summers 1989. The carbon budget in the outer solar nebula. *Icarus* **82,** 1–35.

Simonelli, D. P., and R. T. Reynolds 1989. The interiors of Pluto and Charon: Structure, composition, and implications. *Geo. Res. Lett.* **16,** 1209–1212.

Standish, E. M. 1994. Improved ephemerides of Pluto. *Icarus* **108,** 180–185.

Stern, S. A. 1988. Constraints on Pluto's density and composition. *Icarus* **73,** 269–278.

Stetson, P. B. 1987. DAOPHOT: A computer program for crowded-field stellar photometry. *Publ. Astron. Soc. Pacific* **99,** 191–222.

Stevenson, D. J. 1987. Origin of the Moon: The collisional hypothesis. *Ann. Rev. Earth Planet. Sci.* **15,** 271–315.

Stone, R. C. 1993. Recent advance with the USNO (Flagstaff) transit telescope. In *Developments in Astrometry and Their Impact on Astrophysics and Geodynamics*, (I. I. Mueller and B. Kolaczek, Eds.), IAU Sympos. 156, p. 65. Kluwer, Dordrecht.

Stone, R. C., D. G. Monet, A. K. B. Monet, R. L. Walker, H. A. Ables, A. R. Bird, and F. H. Harris 1996. The Flagstaff Astrometric Scanning Transit Telescope (FASTT) and star positions determined in the extragalactic reference frame. *Astron. J.* **111,** 1721–1742.

Tholen, D. J., and M. W. Buie 1990. Further analysis of the Pluto–Charon mutual event observations—1990. *Bull. Am. Astron. Soc.* **22,** 1129.

Tholen, D. J., and M. W. Buie 1997. The orbit of Charon. I. New Hubble Space Telescope observations. *Icarus* **125,** 245–260.

Wolfram, S. 1991. *Mathematica.* Addison–Wesley, Redwood City, CA.

Young, E. F. 1992. *An Albedo Map and Frost Model of Pluto.* Ph.D. thesis, Massachusetts Institute of Technology.

Young, E. F., and R. P. Binzel 1993. Comparative mapping of Pluto's sub-Charon hemisphere—Three least squares models based on mutual event lightcurves. *Icarus* **102,** 134–149.

Young, L. A., C. B. Olkin, J. L. Elliot, D. J. Tholen, and M. W. Buie 1994. The Charon–Pluto mass ratio from MKO astrometry. *Icarus* **108,** 186–199.